

GENERAL ARTICLE

Epigenetic changes of the thioredoxin system in the tx-j mouse model and in patients with Wilson disease

Charles E. Mordaunt¹, Noreene M. Shibata², Dorothy A. Kieffer², Anna Członkowska³, Tomasz Litwin³, Karl Heinz Weiss⁴, Daniel N. Gotthardt⁴, Kristin Olson⁵, Dongguang Wei⁵, Stewart Cooper⁶, Yu-Jui Yvonne Wan⁵, Mohamed R. Ali⁷, Janine M. LaSalle^{1,*} and Valentina Medici^{2,*}

¹Department of Medical Microbiology and Immunology, Genome Center, and MIND Institute, University of California, Davis, California, USA, ²Department of Internal Medicine, Division of Gastroenterology and Hepatology, University of California, Davis, California, USA, ³Second Department of Neurology, Institute of Psychiatry and Neurology, Warsaw, Poland, ⁴Department of Internal Medicine IV, University Hospital Heidelberg, Heidelberg, Germany, ⁵Department of Pathology, University of California, Davis, California, USA, ⁶California Pacific Medical Center, San Francisco, California, USA and ⁷Department of Surgery, University of California, Davis, California, USA

*To whom correspondence should be addressed at: University of California, Davis Division of Gastroenterology and Hepatology Department of Internal Medicine 4150 V Street, Suite 3500 Sacramento, CA 95817 Office: 916-734-3751; Fax: 916-734-7908; Email: vmedici@ucdavis.edu

Abstract

Wilson disease (WD) is caused by mutations in the copper transporter ATP7B, leading to copper accumulation in the liver and brain. Excess copper inhibits S-adenosyl-L-homocysteine hydrolase, leading to variable WD phenotypes from widespread alterations in DNA methylation and gene expression. Previously, we demonstrated that maternal choline supplementation in the Jackson toxic milk (tx-j) mouse model of WD corrected higher thioredoxin 1 (TNX1) transcript levels in fetal liver. Here, we investigated the effect of maternal choline supplementation on genome-wide DNA methylation patterns in tx-j fetal liver by whole-genome bisulfite sequencing (WGBS). Tx-j *Atp7b* genotype-dependent differences in DNA methylation were corrected by choline for genes including, but not exclusive to, oxidative stress pathways. To examine phenotypic effects of postnatal choline supplementation, tx-j mice were randomized to one of six treatment groups: with or without maternal and/or continued choline supplementation, and with or without copper chelation with penicillamine (PCA) treatment. Hepatic transcript levels of TNX1 and peroxiredoxin 1 (*Prdx1*) were significantly higher in mice receiving maternal and continued choline with or without PCA treatment compared to untreated mice. A WGBS comparison of human WD liver and tx-j mouse liver demonstrated a significant overlap of differentially methylated genes associated with ATP7B deficiency. Further, eight genes in the thioredoxin (TXN) pathway were differentially methylated in human WD liver samples. In summary, *Atp7b* deficiency and choline supplementation have a genome-wide impact, including on TXN system-related genes, in tx-j mice. These findings could explain the variability of WD phenotype and suggest new complementary treatment options for WD.

The authors wish it to be known that, in their opinion, the last two authors should be regarded as joint last authors.

Received: June 2, 2018. Revised: June 2, 2018. Accepted: July 9, 2018

© The Author(s) 2018. Published by Oxford University Press. All rights reserved.

For Permissions, please email: journals.permissions@oup.com

Introduction

Wilson disease (WD) is an autosomal recessive genetic disorder caused by mutations in the copper transporter gene, ATPase copper transporting beta (*ATP7B*) (45). Defects in this protein cause copper accumulation in the liver and brain, leading to hepatic, neurologic and psychiatric symptoms of varying severity (29,44). One of the major challenges posed by WD is the highly varied and unpredictable clinical presentation. Attempts to link the over 500 disease-causing mutations in the *ATP7B* gene (47) to phenotypic presentation have largely been unsuccessful (6,17,37), prompting researchers to investigate other explanations for the heterogeneous manifestations of WD (33).

Epigenetic regulation of gene expression may be one mechanism contributing to the heterogeneity in WD. Epigenetics encompasses a wide range of regulatory processes influencing gene expression without altering the nucleotide sequence. The most well-understood epigenetic mechanism is DNA methylation (22), which involves the addition of methyl groups to cytosine bases, typically at CpG sites (21). This reaction is mediated by three DNA methyltransferases (DNMTs): DNMT1, DNMT3a and DNMT3b. DNMT1 maintains DNA methylation (3), whereas DNMT3a and DNMT3b catalyze *de novo* DNA methylation (42). DNA methylation is highly influenced by the availability of the universal methyl donor S-adenosylmethionine (SAM), most of which is produced in the liver (7). The production of SAM is dependent on the availability of methyl donors (e.g. folate, vitamin B12, methionine, betaine and choline), many of which are influenced by dietary intake and genetic variation in genes related to one-carbon metabolism (40). Copper has been shown to inhibit the activity of S-adenosyl-L-homocysteine hydrolase (SAHH) (23), a key enzyme that regulates the amount of SAM available for methylation reactions. Inhibition of SAHH can ultimately result in impaired methylation (29).

Mitochondria structural (48) and functional (18) abnormalities and accompanying oxidative stress (39), are common features of WD and may be additional key factors contributing to WD heterogeneity. Excess cellular copper can oxidize protein cysteine residues leading to disulfide bond formation (56), which ultimately results in altered protein activity (1). Indeed, proteomics analysis of saliva from WD patients found significantly more proteins with disulfide bonds compared to healthy controls, which the authors concluded was a consequence of the oxidative stress and inflammation that occurs in WD (5). The thioredoxin (TXN) and glutaredoxin pathways protect against oxidative stress by reducing disulfide bonds in proteins (1,43). The cytosolic TXN system consists of thioredoxin 1 (TXN1), which reduces disulfide bonds, and NADPH and thioredoxin reductase 1 (TXNRD1), which act together to return TXN1 to a reduced state (28). The mitochondrial form of the TXN system consists of TXN2 and TXNRD2 (28). Inflammatory conditions, including diabetes (24,27) and ethanol consumption (10), are accompanied by reduced TXN activity and many studies have suggested increasing TXN1 protein expression may be useful in preventing inflammation and neurodegeneration (54).

A deeper analysis of fetal liver transcriptome data previously generated by our group found *Txn1* gene expression to be significantly higher in fetal livers from the Jackson toxic milk (tx-j) mouse model of WD compared to wild-type mice and expression was returned to wild-type levels with 4 weeks of dietary maternal choline supplementation (33). To provide epigenomic context for gene expression changes with *Atp7b* deficiency and choline supplementation, we assessed DNA methylation across

the genome in fetal liver with whole-genome bisulfite sequencing (WGBS) and its association with transcription. In a more focused approach, we tested the hypothesis that dietary supplementation with the methyl donor choline, alone or combined with the copper chelator penicillamine (PCA), alters hepatic expression of genes relevant to DNA methylation and the TXN system in tx-j mice. Data is presented as sexes combined as well as male and female mice separately due to potential sex-driven differences in DNA methylation (26). Additionally, we investigated the DNA methylation profile of genes related to the TXN pathway in tx-j mouse fetal livers and in liver from WD patients compared to healthy control subjects.

Results

Choline affects *Atp7b*-associated methylome and transcriptome changes in fetal liver

To determine if utero choline supplementation could counteract the epigenetic effects of *Atp7b* deficiency, we conducted WGBS on fetal liver from wild-type and tx-j mice prenatally treated with either control or choline diets. We identified differentially-methylated regions (DMRs) that distinguish each group by both *Atp7b* genotype and choline treatment (Fig. 1A, B Mouse DMRs Supplemental Table). Six of these DMRs were identified with a genome-wide significant family-wise error rate (FWER) < 0.05 (Fig. S1). The genes nearby genotype and treatment DMRs identified in this analysis include *Atp7b* itself as well as genes involved in oxidative stress and the TXN pathway, such as *Gpx4*, *Prdx2* and *Hif1 α* (Fig. S2). We further demonstrated the genotype-specific DMRs are corrected with prenatal choline treatment (Fig. 1C, D). Additionally, the methylation changes and genes associated with choline treatment were distinct from those associated with genotype (Fig. S3).

Because DMRs may act long-range, and therefore not necessarily be involved in regulation of their assigned genes, DMR methylation was correlated with gene expression across mouse fetal liver samples to characterize the impact of altered methylation on transcription (Fig. 2A, DMR Meth Exp Assoc Supplemental Table). The expression of DMR genes was further analyzed to identify high-confidence genes whose expression is associated with DMR methylation and associated with changes by genotype and treatment (Fig. 2B). Among the significant associations were *Sept9* and *Tbc1d1* with false discovery rate (FDR) *q*-value < 0.05 (Fig. 2C, D). Other genes associated with DMR methylation included *Uhrf1*, *Mgmt*, *Irs2* and *Axl*.

Atp7b genotype and choline affect methylation and expression of the TXN system in fetal liver

To examine the effect of *Atp7b* mutation and prenatal choline treatment on DNA methylation and gene expression of genes specifically in the TXN system, promoter methylation was extracted from WGBS data and gene expression was assayed by RNA-seq on the same samples (Mouse *Txn* Meth Exp Supplemental Table). This included a deeper analysis of fetal liver transcriptome data previously generated by our group (33). Methylation at *Hif1 α n* and *Gstp1* was associated with *Atp7b* deficiency, while methylation at *Txn2* was associated with choline treatment (Fig. 3A, S4A). TXN system gene expression was much more affected than methylation by *Atp7b* genotype and choline treatment (Fig. 3B, S4B). Fifteen genes in this pathway had a significant main effect of mouse genotype, choline treatment or an interaction between genotype and treatment, including *Hif1 α n*, *Gpx4*, *Prdx2*, *Txn1* and *Txn2* ($P < 0.05$).

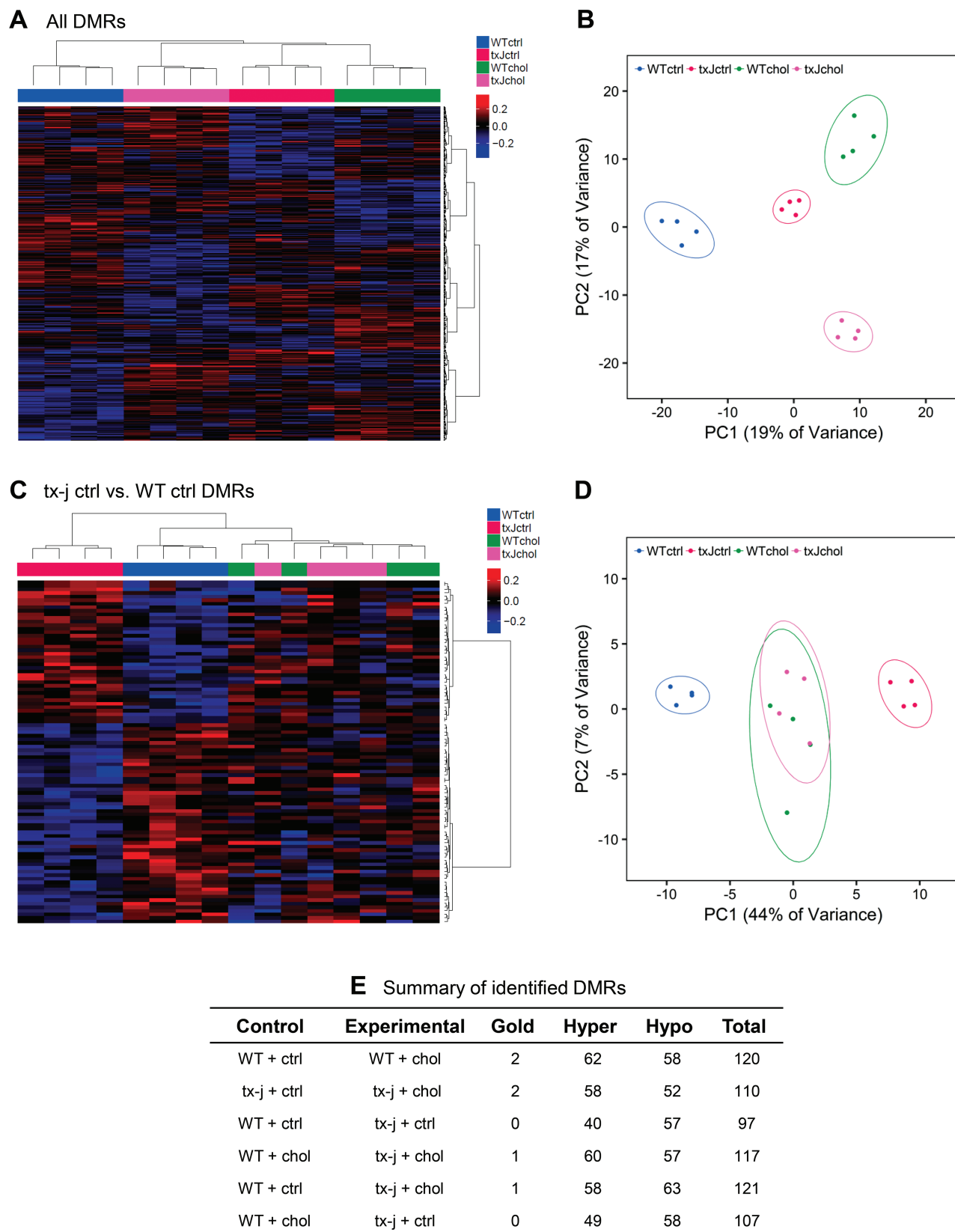


Figure 1. Prenatal choline treatment induces a distinct methylation pattern in mouse fetal liver, including amelioration of *Atp7b* mutation-associated methylation changes. WGBS was performed on DNA from mouse E17 fetal livers and DMRs were identified between tx-j and WT genotypes as well as prenatal choline and control treatments. (A) Hierarchical clustering and heatmap of methylation in DMRs from all comparisons. (B) Principle component analysis of DMR methylation from all comparisons. (C) As in (A), but only DMRs from tx-j ctrl versus WT ctrl comparison. (D) As in (B), but only DMRs from tx-j ctrl versus WT ctrl comparison. (E) Table of DMRs from all comparisons.

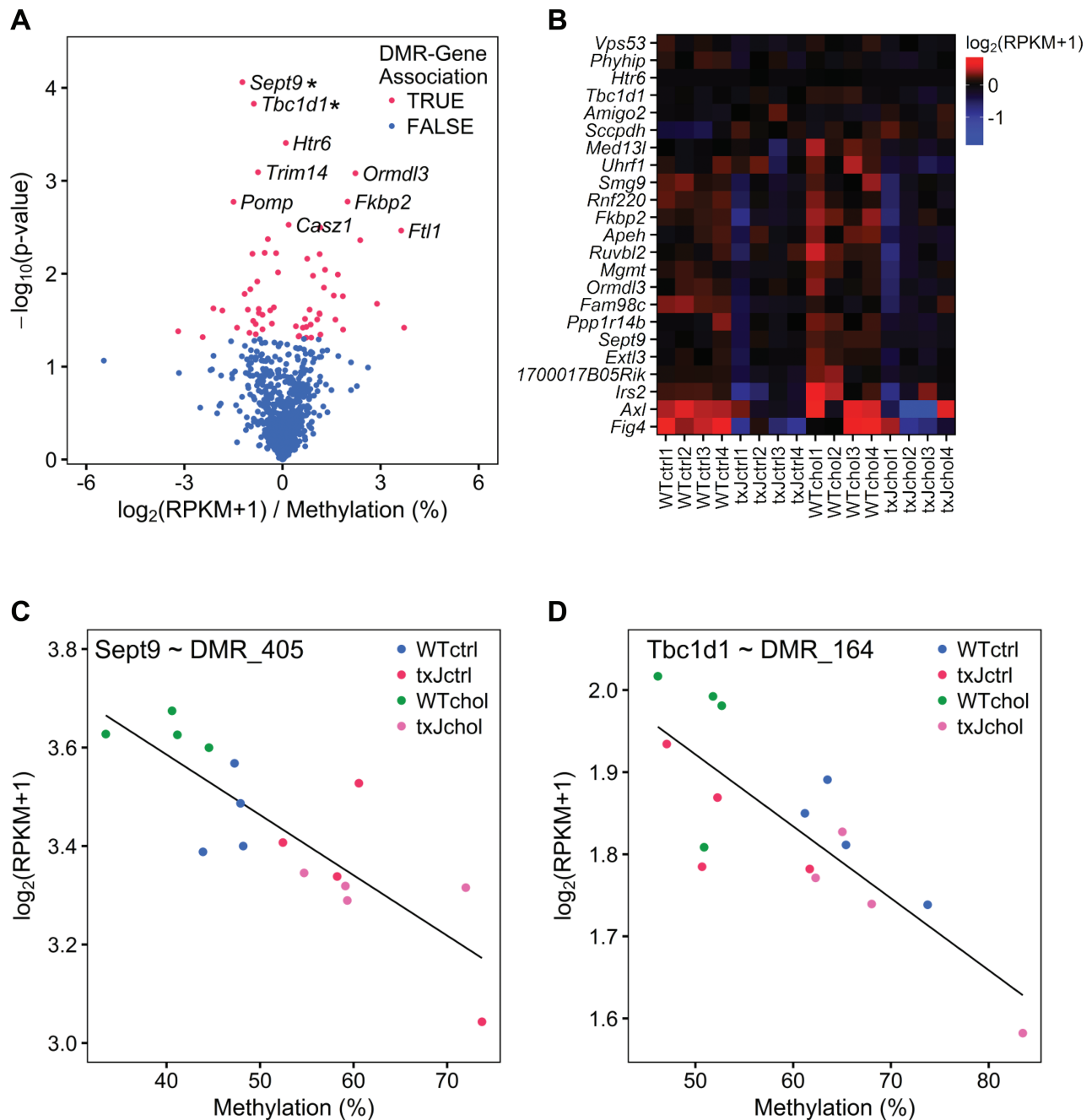


Figure 2. Altered methylation from *Atp7b* mutation and prenatal choline treatment impacts gene expression in mouse fetal liver. RNA-seq and WGBS were performed on the same E17 liver samples. DNA methylation at genotype and treatment DMRs was associated with gene expression by linear regression at genes assigned by GREAT. (A) Volcano plot of DMR methylation and gene expression. DMR-gene associations were called if uncorrected $P < 0.05$. Significant DMR gene associations (*) had FDR q -value < 0.05 . (B) Heatmap of expression of DMR-associated genes with changing expression by genotype and treatment. Main effect of genotype and treatment group on expression was determined by ANOVA $P < 0.05$. Significant association of methylation and gene expression were plotted for (C) *Sept9* and (D) *Tbc1d1*.

Notably, we found significantly higher hepatic transcript levels of *Txn1* in tx-j mice compared to wild-type mice. Four weeks of maternal choline supplementation returned tx-j fetal hepatic *Txn1* levels to that of wild-type mice, suggesting beneficial effects of choline on a key gene in the TXN system.

Response of tx-j mice to dietary treatments

Having established that prenatal choline supplementation was effective at counteracting the in utero epigenetic effects of the

genotype effect, we then sought to determine the prenatal choline supplementation effects in combination with either postnatal choline and/or postnatal PCA chelation treatments on the tx-j liver phenotypes and transcript levels for genes in methylation and oxidative stress pathways. Twenty-four-week-old male and female tx-j mice were divided into six treatment groups (Fig. 4). Male tx-j mice receiving copper chelation with PCA had significantly lower hepatic copper concentrations—38–54% lower compared to D-control/P-control mice (Table 1). In contrast, hepatic copper concentrations did not

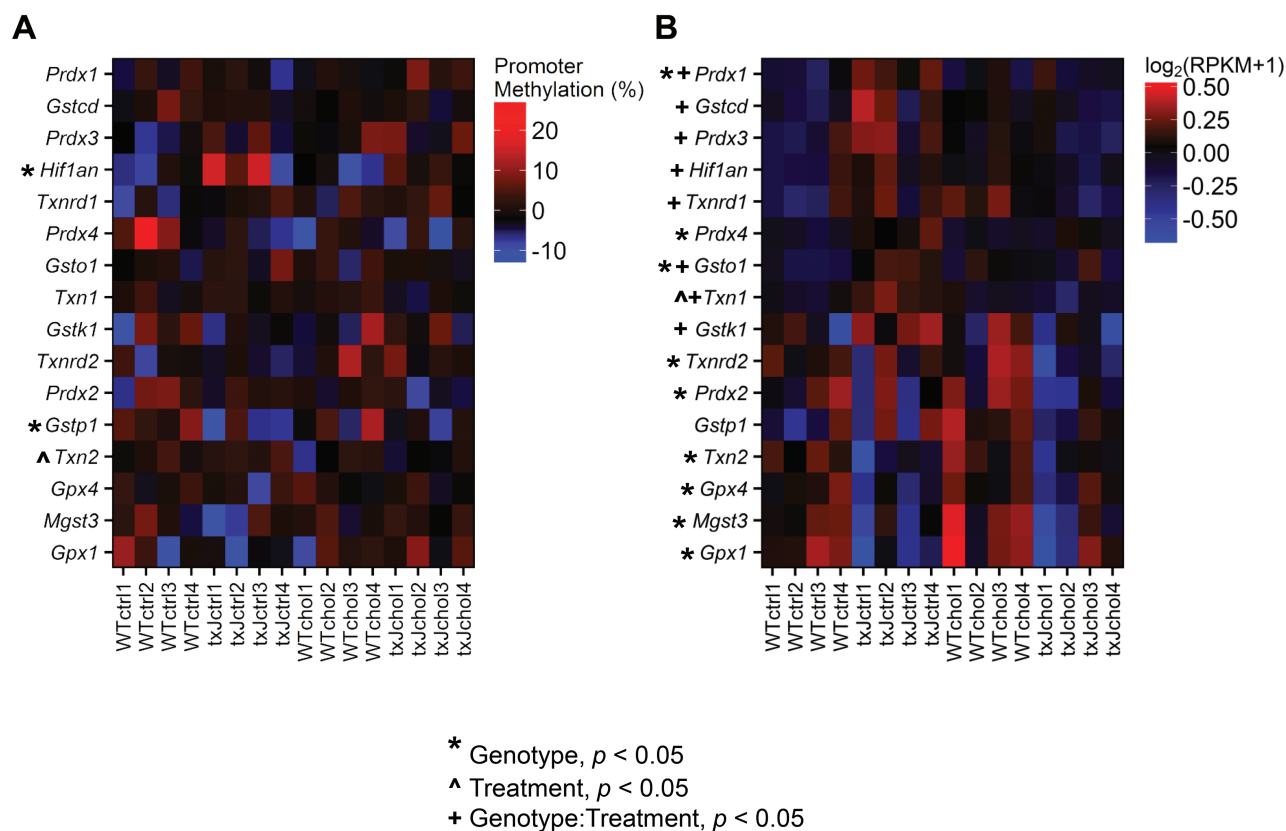


Figure 3. Altered promoter methylation and gene expression at select genes in the TXN system with *Atp7b* genotype and prenatal choline supplementation in mouse fetal liver. RNA-seq and WGBS were performed on the same E17 liver samples. (A) Promoter methylation was determined based on methylated over total reads in the region 5 kb upstream to 1 kb downstream of the transcription start site. Heatmap of promoter methylation at select TXN system genes is plotted for each sample relative to the average for each region. (B) Heatmap of gene expression is plotted for each sample relative to the average for each gene. For methylation and expression, significance was determined by two-way ANOVA with mouse genotype and choline treatment as independent variables, followed by Tukey's Honest Significant Difference post hoc test. Significant changes were called if uncorrected $P < 0.05$.

change after PCA copper chelation in female tx-j mice. Hepatic copper was significantly higher in female mice compared to male mice in all treatment groups except D-control/P-control; however, some positive effects of PCA treatment were observed in female tx-j mice regardless of control or choline-supplemented diets, including lower liver-to-body weight ratio, lower plasma alanine transaminase (ALT) levels and reduced hepatic inflammation on histology (Table 1 and Fig. 5). Liver protein carbonyl concentrations, as an indicator of disulfide bond formation, were significantly higher in male, but not female, D-control/P-control+PCA compared to D-control/P-control tx-j mice (Table 1). A subgroup of female mice receiving 2XPCA did not show any differences in hepatic copper, ALT levels and key gene expression compared to female mice receiving normal PCA (Supplemental Table 1).

Liver histology revealed significantly more steatosis in D-choline/P-control+PCA males compared to other male mice (Fig. 5), whereas steatosis did not differ among female mice. Inflammation did not differ among male mice across all treatment groups; in female mice, PCA effectively reduced inflammation. Inflammation was greater in males receiving PCA treatment compared to females from the same treatment group as demonstrated by the presence of more inflammatory loci with neutrophils. No fibrosis was observed in any histological samples (data not shown).

Transcript levels of genes related to TXN are affected by sex and diet in tx-j mice

Hepatic transcript and protein levels of *Txn1* were highest in mice receiving both maternal and continued choline treatment with or without PCA in both sexes (D-choline/P-choline and D-choline/P-choline+PCA; Fig. 6). Increased TXN1 levels after choline treatment were also confirmed by ELISA (Supplemental Table 2). *Txn2* displayed changes similar to *Txn1* though there were no significant differences among any treatment groups in the males (Fig. 6). *Txnrd1* hepatic gene expression was significantly higher in D-control/P-control female mice compared to all other treatment groups.

Prdx1, another transcript in the TXN system, was found to be higher in fetal tx-j livers compared to wild-type mice and normalized by maternal choline supplementation (Fig. 3B). When studied in adult mouse livers, *Prdx1* gene expression was significantly higher in D-choline/P-choline male and female mice (Fig. 6).

Transcript levels of genes related to DNA methylation are affected by sex and diet in tx-j mice

Dnmt1 hepatic transcript levels were significantly affected by choline and PCA with lower expression in D-choline/P-choline and all PCA-treated mice compared to D-control/P-control and D-choline/P-control in both sexes (Fig. S5). In contrast,

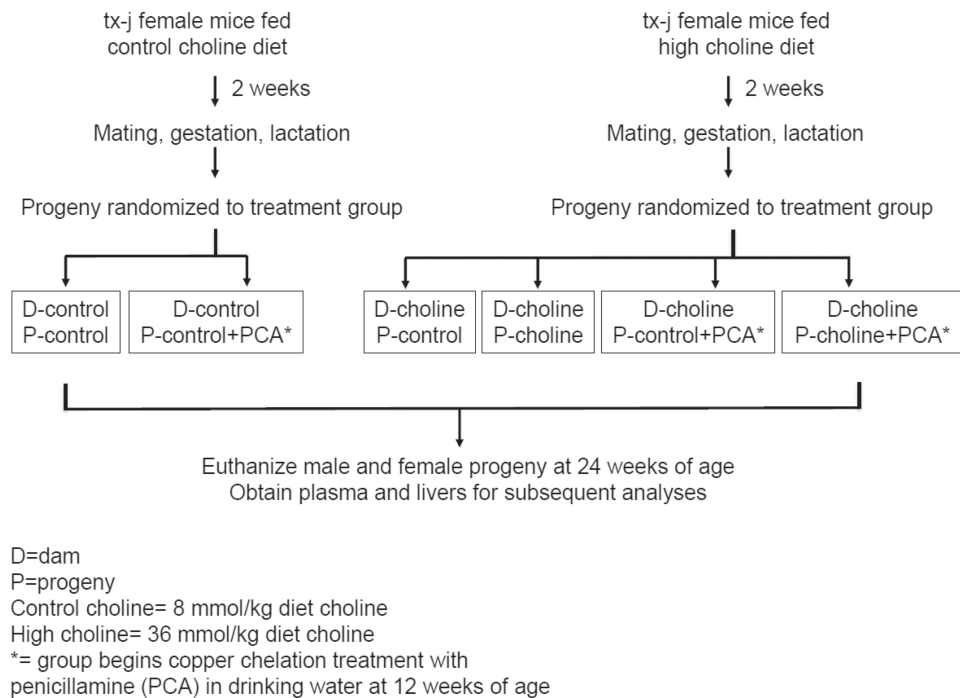


Figure 4. Mouse study design. Tx-j dams were fed diets with or without choline supplementation 2 weeks before mating and throughout gestation and lactation. Tx-j progeny were weaned and continued on diets with or without choline supplementation. Subgroups of tx-j progeny on each diet were given penicillamine treatment from 12 to 24 weeks of age.

Dnmt3a hepatic gene expression was not significantly different among treatment groups of either sex. Similarly, *Dnmt3b* hepatic gene expression revealed little difference among treatment groups except three groups of males (D-control/P-control; D-control/P-control+PCA; D-choline/P-control+PCA) who showed higher expression than their female counterparts. *Sahh* hepatic gene expression was significantly higher than control in four groups of females (D-choline/P-control; D-choline/P-choline; D-control/P-control+PCA; D-choline/P-choline+PCA), with D-choline/P-choline+PCA the most efficient at increasing *Sahh* transcript levels.

Correlations between liver histology and genes related to DNA methylation and the TXN system

To identify relationships between liver histopathological indices and hepatic expression of genes related to DNA methylation and the TXN system, cross-correlation plots were created and revealed significant correlations among liver histology and hepatic gene expression measurements in male and female tx-j mice (Fig. S6). Both male and female mice displayed a negative correlation between *Dnmt1* and *Txn2* hepatic gene expression and a positive correlation between *Sahh* and *Txn2* hepatic gene expression. Female mice displayed positive correlations between *Dnmt1* and the liver-to-body weight ratio, histological inflammation and plasma ALT; only the liver-to-body weight ratio correlation was also seen in male mice. Hepatic copper and iron concentrations were significantly positively correlated in male, but not female, tx-j mice. However, there was a significant positive correlation between liver protein carbonyl concentrations and hepatic gene expression of *Txnrd1* and *Prdx1* only in female tx-j mice, while both sexes showed a positive correlation between *Txn* expression and liver protein carbonyl concentrations.

Mouse *Atp7b* mutation and choline supplementation methylation changes are shared with human WD patients

To assess the clinical relevance of methylation changes in mice, genes nearby mouse fetal liver *Atp7b* genotype and choline treatment DMRs were overlapped with genes nearby human liver WD-specific DMRs, which distinguish WD patients from healthy controls (Fig. 7, Mouse Human Overlap Supplemental Table). Nearly all mouse comparisons significantly overlapped with human WD DMRs (FDR q -value < 0.05). Interestingly, 34 genes were differentially methylated in the same direction with *Atp7b* genotype in mouse and human (Hypermethylated: q -value = 0.01; Hypomethylated: q -value = 3.0E-6); these included *Sept9*, *Alkbh5*, *Cebpb*, *Mlxipl* and *Sh3pxd2a*, suggesting that *Atp7b* deficiency results in conserved methylation changes in liver between human and mouse. TXN system genes also had altered methylation at the promoter regions in liver biopsies of WD patients compared to healthy controls (Fig. 8, S7, Human *Txn* Meth Supplemental Table). *GSTZ1*, *MGST1*, *PRDX1* and *TXN2* were hypermethylated, while *GSTM2*, *GSTM5*, *GSTP1* and *MGST3* were hypomethylated in WD patients. Notably, *Gstp1* was also hypomethylated in tx-j mice (Fig. 3A). Together, these results suggest a conserved dysregulation of methylation in TXN system genes with *Atp7b* deficiency in mice and humans.

Discussion

The lack of genotype–phenotype correlations in WD (6,17,37) indicates factors other than genetics, such as epigenetics, play a role in disease presentation and progression. The current study uncovered several novel findings related to WD. First, in the tx-j mouse model of WD, perinatal choline supplementation

Table 1 . Effects of diet treatments on mouse body and liver weight, hepatic copper and iron as well as plasma ALT

MALES	D-control	D-choline	D-choline	D-control	D-choline	D-choline
	P-control	P-control	P-choline	P-control +PCA	P-control +PCA	P-choline +PCA
	(n = 4)	(n = 10)	(n = 5)	(n = 3)	(n = 10)	(n = 5)
Body weight (g)	31.4 ± 2.4	32.9 ± 1.1	33.3 ± 0.5 [#]	35.3 ± 1.5 [#]	31.7 ± 1.5	32.0 ± 1.7
Liver per body weight	0.0508 ± 0.0009	0.0488 ± 0.0012	0.0494 ± 0.0015	0.0493 ± 0.0026 [#]	0.0460 ± 0.0014 [#]	0.0484 ± 0.0022 [#]
Copper (µg/g)	42.0 ± 1.3 ^a	42.9 ± 0.8 ^{a#}	39.7 ± 0.5 ^{a#}	19.3 ± 4.2 ^{b#}	26.1 ± 2.3 ^{b#}	22.4 ± 1.1 ^{b#}
Iron (µg/g)	53.8 ± 2.3 ^{ab#}	54.6 ± 1.3 ^{a#}	53.7 ± 2.4 ^{ab#}	39.6 ± 6.2 ^{b#}	45.9 ± 2.3 ^{ab#}	46.0 ± 3.4 ^{ab#}
Protein carbonyl (nmol/mg)	2.68 ± 0.24 ^a	3.03 ± 0.37 ^{ab}	3.92 ± 0.23 ^{ab}	4.59 ± 0.79 ^b	3.43 ± 0.10 ^{ab}	3.77 ± 0.41 ^{ab}
Plasma ALT (U/l)	65.5 ± 12.4 [#]	68.7 ± 3.8 [#]	59.8 ± 7.7 [#]	96.6 ± 1.0 [#]	89.5 ± 7.7 [#]	78.8 ± 9.1 [#]
FEMALES	D-control	D-choline	D-choline	D-control	D-choline	D-choline
	P-control	P-control	P-choline	P-control +PCA	P-control +PCA	P-choline +PCA
	(n = 10)	(n = 6)	(n = 5)	(n = 6)	(n = 7)	(n = 5)
Body weight (g)	30.6 ± 1.9	32.6 ± 1.0	28.0 ± 1.8 [#]	29.4 ± 1.3 [#]	30.6 ± 2.1	32.2 ± 2.5
Liver per body weight	0.0559 ± 0.0018 ^a	0.0510 ± 0.0015 ^a	0.0534 ± 0.0022 ^a	0.0430 ± 0.0012 ^{b#}	0.0409 ± 0.0015 ^{b#}	0.0418 ± 0.0010 ^{b#}
Copper (µg/g)	47.0 ± 1.6	47.3 ± 1.2 [#]	46.8 ± 1.2 [#]	45.9 ± 1.8 [#]	49.8 ± 2.0 [#]	48.9 ± 2.3 [#]
Iron (µg/g)	44.6 ± 1.4 ^{a#}	45.0 ± 2.3 ^{a#}	43.8 ± 1.4 ^{a#}	62.0 ± 3.2 ^{b#}	57.6 ± 1.5 ^{b#}	60.3 ± 1.6 ^{b#}
Protein carbonyl (nmol/mg)	3.14 ± 0.43	3.03 ± 0.23	4.04 ± 0.44	3.09 ± 0.32	3.23 ± 0.08	3.64 ± 0.41
Plasma ALT (U/l)	41.7 ± 4.5 ^{ab#}	47.7 ± 3.4 ^{a#}	37.3 ± 4.9 ^{ac#}	20.1 ± 4.6 ^{c#}	25.9 ± 4.9 ^{bc#}	17.4 ± 1.9 ^{c#}

Values are expressed as mean ± SEM.

Values with different letter symbols are significantly different from each other.

Values with a hashtag (#) are significantly different between sexes of the same group.

D, dam; P, progeny.

corrected the genotype effects on DNA methylation differences in fetal liver. Second, perinatal maternal with continued choline supplementation increased transcript and protein expression of *Txn1*, an important mediator of anti-oxidative responses in the TXN system. Changes in the TXN system were observed from fetal to adult life. Third, we translated these findings to WD in humans, showing a significant overlap in genes with altered DNA methylation levels between the tx-j mouse and human WD liver genome-wide, and specifically in genes relevant to the TXN system.

Current treatment options for WD, including zinc salts and copper chelators, are used with variable success and can be accompanied by many side effects (13,50). There is a need for additional adjunctive or stand-alone therapies that are safe and effective; dietary choline supplementation is one potential option. Choline is synthesized in the body *de novo*; however, the amount produced is not adequate to support the body's needs and must therefore be obtained in the diet (4). Choline is used in methylation reactions (e.g. synthesis of the universal methyl donor, SAM), which may be particularly important in WD because copper inhibits SAHH (23), a key enzyme regulating the amount of SAM available for methylation reactions. Furthermore, choline has been shown to modulate fatty liver development (16) and inflammation (14,36) in humans—both of which are also common findings in WD (11,46). Finally, during pregnancy the demand for choline greatly increases to support fetal growth and development (55). Our results suggest that

providing sufficient dietary choline during pregnancy and early postnatal life may be important in preventing the more severe WD symptoms in adulthood.

Protein disulfide bond formation is one consequence of copper-induced oxidative stress (5). Disulfide bonds occur when the thiol groups of two cysteine protein residues become oxidized forming a covalent bond (1). The TXN system is one of two pathways primarily responsible for reducing disulfide bonds and maintaining redox balance (28). We found hepatic gene expression of *Txn1* and *Txn2*, components of cytosolic and mitochondrial TXN systems, to be upregulated in adult tx-j mice receiving maternal and continued choline supplementation. Increased *Txn* expression is considered beneficial for inflammatory conditions (31,54) and therapeutic strategies to elevate its expression are being investigated for the treatment of many diseases, including metabolic syndrome and neurodegeneration (30). *Prdx1* hepatic gene expression showed the same pattern as *Txn1*; TXN and PRDX work together to maintain redox status—TXN reduces the oxidized form of PRDX, and reduced PRDX in turn scavenges reactive oxygen species, such as hydrogen peroxide (19). In contrast, *Txn1* and *Prdx1* gene expression in fetal liver was highest in control tx-j compared to wild-type or choline-treated tx-j mice. This opposing *Txn1* and *Prdx1* response between fetal and adult tx-j mice might be related to hepatic copper levels as fetal tx-j livers exhibit copper deficiency, not excess (34). The lower transcript levels of *Txn1* and *Prdx1* in untreated adult tx-j mice and hypermethylation of TXN-related

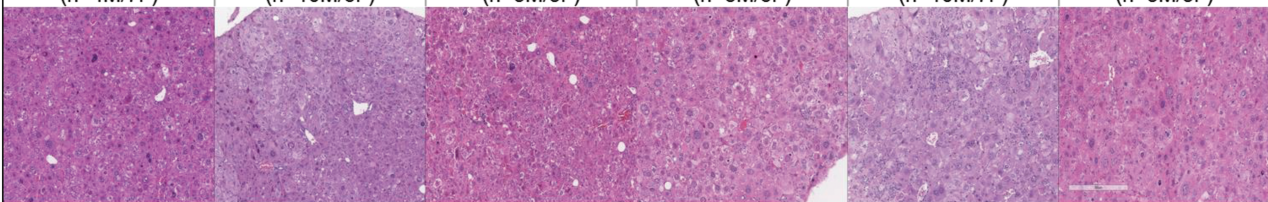
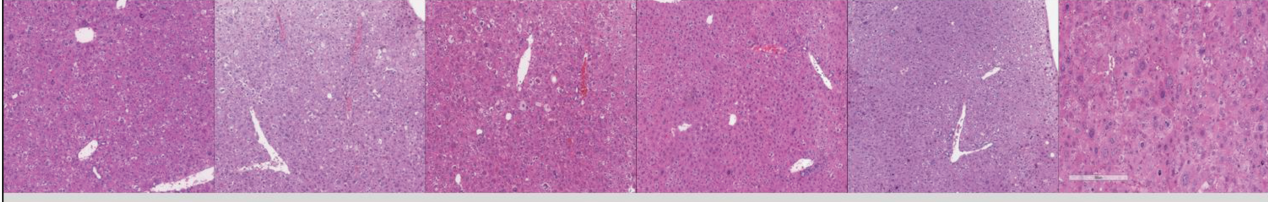
D-control P-control (n=4M/7F)	D-choline P-control (n=10M/6F)	D-choline P-choline (n=5M/5F)	D-control P-control+PCA (n=3M/6F)	D-choline P-control+PCA (n=10M/7F)	D-choline P-choline+PCA (n=5M/5F)
					
Steatosis (males)					
1.8 ± 0.3 ^a	2.1 ± 0.1 ^{ab}	1.6 ± 0.2 ^a	2.3 ± 0.3 ^{ab}	2.8 ± 0.2 ^{b#}	2.0 ± 0.0 ^{ab}
Inflammation (males)					
1.0 ± 0.4	1.5 ± 0.2 [#]	1.6 ± 0.2	2.0 ± 0 [#]	1.5 ± 0.3	2.0 ± 0.3 [#]
% samples with inflammatory loci containing 1 or more neutrophils (males)					
25%	80%	0%	100%	80%	60%
					
Steatosis (females)					
1.9 ± 0.3	1.7 ± 0.2	2.0 ± 0.0	1.5 ± 0.2	1.3 ± 0.2 [#]	1.2 ± 0.4
Inflammation (females)					
1.6 ± 0.2 ^a	1.3 ± 0.2 ^{ab#}	1.8 ± 0.2 ^a	0.3 ± 0.2 ^{c#}	0.7 ± 0.3 ^{bc}	1.0 ± 0 ^{ac#}
% samples with inflammatory loci contain 1 or more neutrophils (females)					
29%	33%	20%	0%	29%	0%

Figure 5. Effects of diets on mouse liver histology. Values are expressed as mean ± SEM. The number of mice in each group is indicated in parentheses. Values with different letter symbols are significantly different from each other. Values with a hashtag (#) are significantly different between sexes of the same group. Uncorrected $P < 0.05$ considered significant. D, dam; P, progeny.

genes in liver of WD patients compared to healthy controls suggest altered DNA methylation of oxidative response genes may play a role in WD presentation and progression.

Atp7b genotype and maternal choline supplementation affected DNA methylation and expression of genes beyond the TXN system in fetal liver. Overall, 672 DMRs near 1040 genes changed in methylation with *Atp7b* deficiency and/or choline treatment. Among the genes differentially methylated in tx-j compared to WT mice was *Atp7b* itself. Specifically, *Atp7b* was hypermethylated in tx-j fetal liver at its 3' end, which is downstream of the tx-j G712D missense mutation in exon 8 (12), in a potential epigenetic feedback mechanism. *Atp7b* genotype DMR genes in mouse significantly overlapped with differentially methylated genes in human WD liver samples, supporting the tx-j mouse as an appropriate model for epigenetic dysregulation in WD. Notably, *Sept9* was hypomethylated with *Atp7b* deficiency in both mouse and human liver. *Sept9* expression was also significantly negatively associated with methylation at its transcription start site in fetal liver, suggesting that increased *Sept9* expression is a long-term functional consequence of *Atp7b* deficiency. Interestingly, *Sept9* has previously been found to play a role in protecting against fibrogenesis in hepatic stellate cells (53). Only 2 of the 173 genes differentially methylated in tx-j and WT mice were still different between tx-j and WT mice

treated with choline. Additionally, 13 genes hypomethylated in tx-j versus WT were hypermethylated in tx-j with choline supplementation compared to tx-j without choline. Of these 13 genes with improved methylation profiles, 6 were also hypomethylated in human WD patients, including *Afp1*, *Cacnb1*, *Elfn1*, *Mad1l1*, *Psap1* and *Trim11*. Together, this suggests maternal choline supplementation ameliorated genotype-associated methylation differences in mouse fetal liver and may have potential as a complementary treatment for WD.

We observed extensive differences between sexes, both in response to PCA treatment and to choline supplementation. Several studies report different clinical presentation and course between male and female patients with WD (25,15). Whereas these differences were always attributed to hormone levels, it is possible that nutritional factors affecting DNA methylation status could also contribute to these differences. Of note, iron hepatic levels were about 15% lower in female mice compared to their male counterparts in groups without PCA. Even though the biological significance of mildly lower hepatic iron levels in female mice is questionable, we adjusted gene transcript levels using hepatic iron as a covariate and TXN levels were still significantly increased after choline supplementation. Other published studies indicate a close relationship between sex, inflammation and epigenetic mechanisms of gene expression regulation

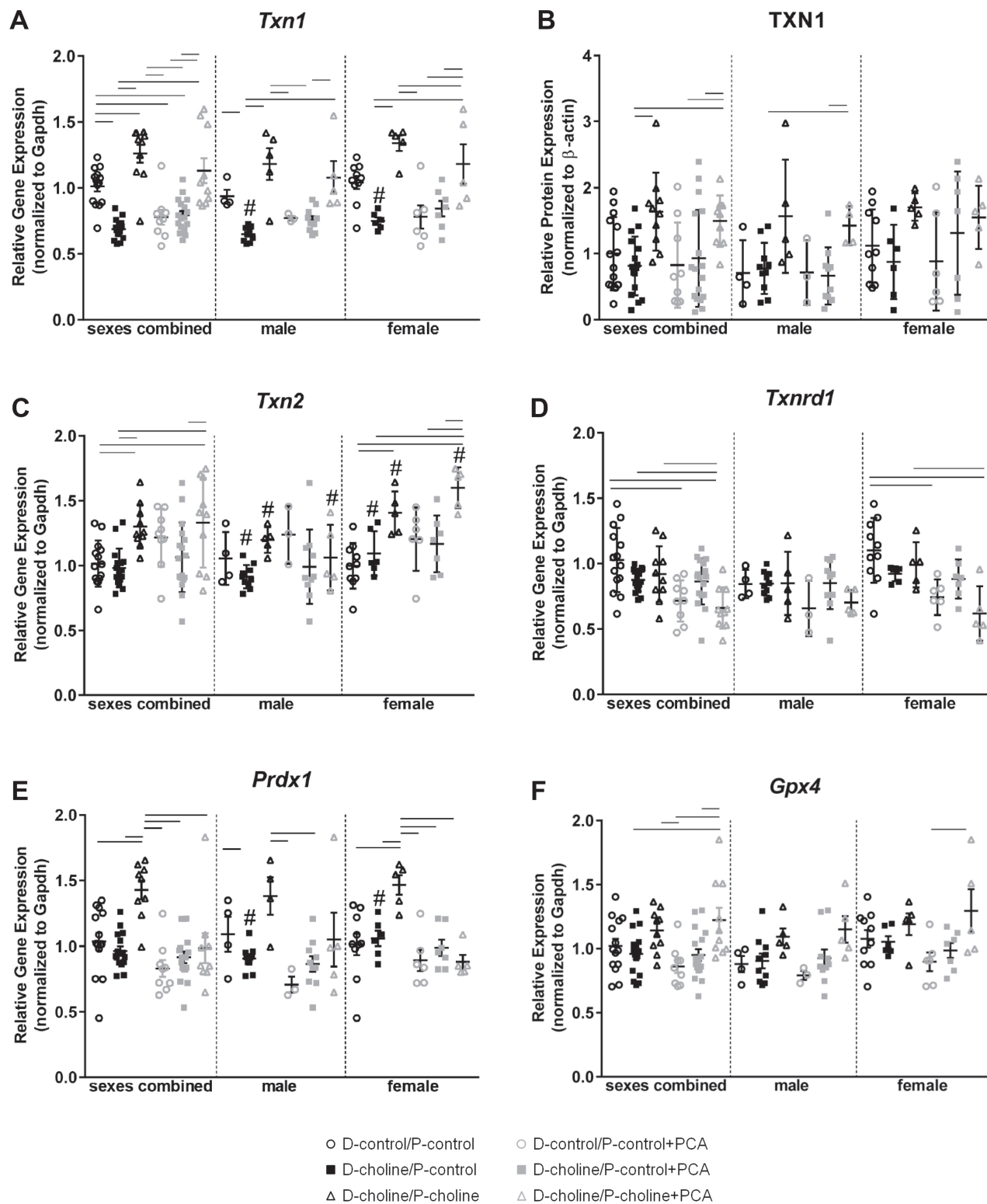
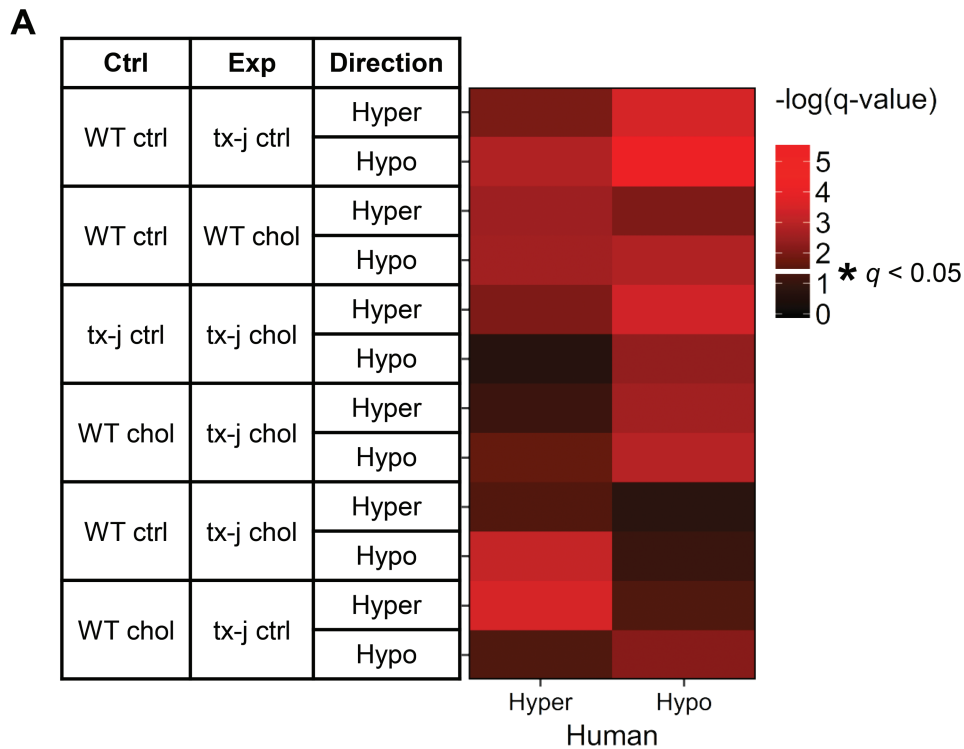


Figure 6. Mouse transcript levels of genes representative of the TXN system. (A, C–F) Gene expression data are normalized to *Gapdh* (9–17 mice/group). (B) Protein expression data for TXN1 are normalized to β -actin. Results are expressed as mean \pm SEM; $P < 0.05$ considered significant. Between-group differences were analyzed by one-way ANOVA; groups with a bar are significantly different from each other. Differences between sexes in the same treatment group were analyzed by Student's *t*-test; values with a hashtag (#) are significantly different between sexes. Using ANCOVA and adjusting for hepatic iron as a covariate, *Txn1* transcript levels were still significantly increased in response to choline supplementation ($P < 0.05$, not shown). D, dam; P, progeny.



B *Atp7b*-Associated Differentially-Methylated Genes in Mouse and Human

Hypermethylated		Hypomethylated		
Odds ratio = 2.53		Odds ratio = 4.07		
q-value = 0.01		q-value = 3.0E-6		
<i>Alkbh5</i>	<i>Sh3pxd2a</i>	<i>Afap1</i>	<i>Hlcs</i>	<i>Sim2</i>
<i>Cebpb</i>	<i>Tmem184a</i>	<i>Aff3</i>	<i>Lonrf2</i>	<i>Tab1</i>
<i>Grid2ip</i>	<i>Zfp750</i>	<i>B4galnt4</i>	<i>Mad111</i>	<i>Tpsg1</i>
<i>Kdelr2</i>		<i>Cacna1h</i>	<i>Myt1l</i>	<i>Trim11</i>
<i>Mink1</i>		<i>Cacnb1</i>	<i>Ppcdc</i>	<i>Wnt11</i>
<i>Mlxipl</i>		<i>Camk2b</i>	<i>Prkcz</i>	<i>Ykt6</i>
<i>Myo15</i>		<i>Elfn1</i>	<i>Psapl1</i>	<i>Zfp644</i>
<i>Ptpn1</i>		<i>Fam129b</i>	<i>Sept9</i>	

Figure 7. Mouse *Atp7b* mutation and prenatal choline treatment DMR genes are shared with human patients with WD. Genes assigned to mouse fetal liver genotype and treatment DMRs by GREAT were overlapped with DMR genes from human WD patient liver biopsies. (A) Heatmap of $-\log(q\text{-value})$ for overlap by direction. Significance was determined by hypergeometric test compared to background genes. (B) Genes with differential methylation in livers of tx-j versus WT mice and WD versus healthy control human subjects. Hypermethylated genes have higher methylation in tx-j mice and WD human subjects, while hypomethylated genes have lower methylation in tx-j mice and WD human subjects.

(2,41,52). This relationship between sex and inflammation has also been shown in liver diseases (8). Notably, there are well-described sex-dependent differences in disease susceptibility that appear to originate from fetal and neonatal environmental exposures (49).

Previous work from our group showed untreated tx-j mice have altered hepatic protein, transcript and metabolite levels relevant to DNA methylation compared to wild-type mice or tx-j mice receiving dietary methyl donor supplementation (33–35). The higher levels of *Dnmt1* and lower levels of *Sahh* hepatic

transcripts in control tx-j mice compared to mice treated with maternal and continued choline supplementation or PCA are in agreement with our previous study (35). Interestingly, in response to choline supplementation, *Txn2* and *Sahh* transcript levels increased more significantly in female compared to male mice and strongly correlated with each other. These findings indicate that females with WD may benefit more from choline supplementation given a better response of methionine metabolism. Results from the present study demonstrate maternal and continued choline supplementation may be an

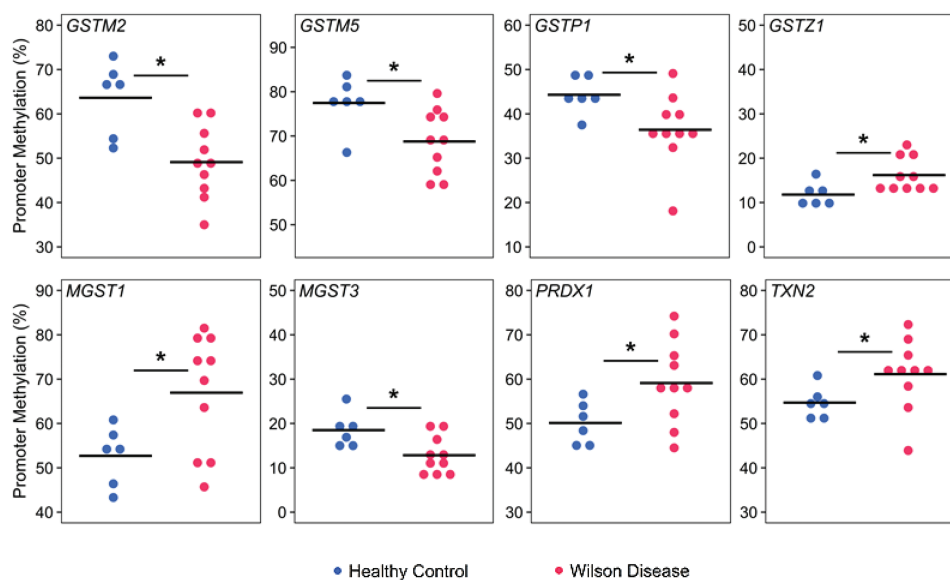


Figure 8. Altered promoter methylation at select genes in the TXN pathway in liver biopsies of patients with WD. WGBS was performed on DNA from liver biopsies of healthy control ($n = 6$) and WD ($n = 10$) subjects. Promoter methylation was determined based on methylated over total reads in the region 5 kb upstream to 1 kb downstream of the transcription start site. Methylation at the promoter of select TXN pathway genes is plotted for each sample. Significance was determined by Student's *t*-test ($P < 0.05$).

effective strategy to recover the impaired DNA methylation observed in *tx-j* mice. A working model showing how WD may be impacted by choline supplementation is presented in Figure 9.

One potential limitation of this study was the absence of a wild-type control group in the postnatal choline treatment design (33). However, the specific intent of the current study was to determine the effects of choline, alone or in combination with PCA, on the disease state in *tx-j* mice. Since our previous studies have established wild-type baseline values for many of the parameters measured in the current study (34,35), we felt that it is unnecessary to repeat these measurements and instead chose to eliminate the group thereby reducing extraneous animal use. In addition, the human study portion is limited by the small sample size. Finally, *Txn* functions beyond disulfide bond reduction, including stimulation of cell growth, inhibition of apoptosis, activation of several transcription factors and regulation of the immune system (28); these additional roles were not explored in the present study and may impact the WD phenotype. Despite these limitations, further research investigating the relationship between WD, choline supplementation and TXN is warranted to explore the potential role of choline as adjunctive treatment for WD. In conclusion, choline, either alone or combined with PCA treatment, may be an effective strategy to combat the copper-induced oxidative stress (39) and cytosolic (23) and mitochondrial protein dysfunction (18), which may improve hepatic presentation and progression of WD.

Materials and Methods

Mice and diets

Wild-type (C3HeB/FeJ) and *tx-j* (C3HeB/FeJ-*Atp7b*<*tx-j*>/J) mouse colonies were maintained at 20–23°C, 45–65% relative humidity and a light cycle of 14 h light/10 h dark. Mice were

maintained on LabDiet 5001 chow. Mice were conventionally housed, 3–4 mice per cage, in open-top cages with TEK-Fresh bedding (Envigo) mixed with PAPERCHIP bedding (Shepherd Specialty Papers). All mouse protocols followed the guidelines of the American Association for Accreditation of Laboratory Animal Care and were reviewed and approved annually by the UC Davis Institutional Animal Care and Use Committee. All animals received humane care according to the criteria outlined in the 'Guide for the Care and Use of Laboratory Animals Eighth Edition' prepared by the National Research Council and published by the National Academy of Sciences in 2011.

Female *tx-j* dams used for this study were switched to AIN-76A purified diet (Dyets, Inc.) containing high choline (36 mmol/kg diet) or normal choline (8 mmol/kg diet) for 2 weeks before mating. For fetal liver experiments, dams continued to consume experimental diets throughout gestation and fetal livers were collected and flash-frozen at embryonic day 17 (E17); since the size of a single mouse fetal liver would severely limit the number of measurements performed, fetal livers from a single dam were pooled at harvest, males and females combined (i.e. 1 fetal liver sample = pooled male and female fetal livers from 1 litter). For experiments in 24-week-old mice, dams consumed experimental diets 2 weeks before mating and throughout gestation and lactation. The copper concentration in *tx-j* mouse milk is insufficient to maintain neonatal growth and development beyond an average of 10 days; therefore, all *tx-j* pups were fostered between day 0 and day 5 post-partum (day 3 average) to a lactating wild-type dam fed the same diet as the *tx-j* dam and that gave birth on or close to the same day as the *tx-j* dam. At weaning, progeny were placed on the appropriate experimental diet for the duration of the study (Fig. 4). To validate the mutant status of our *tx-j* mouse colony, the UC Davis Mouse Biology Program genotyped 3 random mice/treatment group (total $n = 18$ mice) via Taqman allelic discrimination assay and the homozygous mutant status was confirmed in all cases.

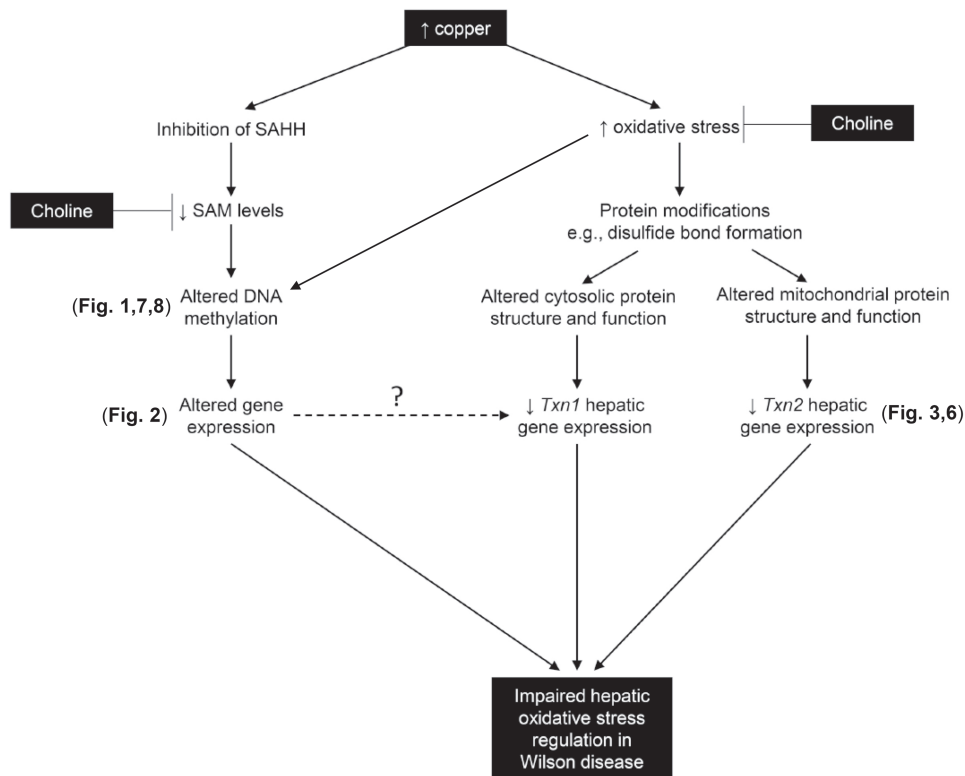


Figure 9. Working model showing how WD may be impacted by choline supplementation.

Progeny (P) from dams (D) fed a normal choline diet were randomized to one of the following treatment groups: (1) D-control/P-control (control); (2) D-control/P-control+PCA. Progeny from dams fed a high choline diet were randomized to one of the following treatment groups: (3) D-choline/P-control; (4) D-choline/P-control+PCA; (5) D-choline/P-choline; (6) D-choline/P-choline+PCA. Group 1 was used as a relative control group. Oral PCA treatment was started at 12 weeks of age and continued through the end of the study. D-penicillamine (Sigma) was dissolved in deionized water and administered at 100 mg/kg b.w./day (35) or 200 mg/kg b.w./day to a subgroup of female mice. Food and deionized water were provided *ad libitum*. Historic records taken from multiple cages over three time points indicate food and water intake does not differ among treatment groups and does not change when PCA treatment is given. Average food intake per mouse was 3 grams/day and average water intake was 3 mL/day.

Non-fasted mice were anesthetized via isoflurane at 24 weeks of age. Approximately 1 mL of blood was collected from the retro-orbital sinus followed by euthanasia via cervical dislocation. Livers were harvested and sections from each liver were either placed in formalin for subsequent blocking in paraffin or flash-frozen in liquid nitrogen and stored at -80°C for further analysis.

RNA isolation from mouse liver

Total RNA was isolated from mouse liver using the RNeasy Mini Kit (QIAGEN). The concentration and purity of samples was determined by measuring the absorbency at A230, A260 and A280 on a NanoDrop spectrophotometer (Thermo Scientific). RNA integrity was further evaluated by agarose gel electrophoresis. Total RNA was stored at -80°C until further use.

cDNA synthesis and quantitative real-time PCR

Reverse transcription was carried out using 5 μg of total RNA and following the protocol provided for the SuperScript III First-Strand cDNA Synthesis kit (Invitrogen). Primers for mouse cDNA sequences were designed using Primer Express 3.0 (Applied Biosystems) or NCBI Primer-BLAST (<http://www.ncbi.nlm.nih.gov/tools/primer-blast/>) and blasted against the mouse genome using NCBI blast to check primer specificity (<http://blast.ncbi.nlm.nih.gov/Blast.cgi>). The amplification efficiency (E) of all assays was calculated from the slope of a standard curve generated via 10-fold serial dilution of pooled control cDNA using the formula $E = 10^{-(1/\text{slope})} - 1$. Primer sequences used are listed in Supplemental Table 3.

Transcriptome analysis by RNA-sequencing

RNA-sequencing of mouse fetal liver was previously described (33). Briefly, 16 samples were chosen from wild-type and tx-j dams receiving control and choline-supplemented diets ($n = 4$ per group, 6–9 pooled fetal livers per sample). Libraries were constructed using the TruSeq Stranded mRNA Sample Preparation kit (Illumina, Inc.). Libraries were sequenced at 8 per lane on the HiSeq 2000 (Illumina, Inc.) at the Vincent J. Coates Genomics Sequencing Laboratory at UC Berkeley.

Sequence paired-end reads (100 bp) were assembled against the annotated mouse reference genome (release 76) (ftp://ftp.ensembl.org/pub/release-76/genbank/mus_musculus/). Data were normalized by calculating the reads per kilo base per million mapped reads, or RPKM, for each gene (38). To select expressed genes, a threshold of RPKM ≥ 0.2 in at least one treatment group was used (51).

Normalization and transformation of data were performed to transform the expression data from negative binomial distribution to normal distribution. Differential expression analysis was performed using t-test ($P \leq 0.05$ and fold change ≥ 1.2) on transformed data to identify genes with significant change in expression between the two genotypes (wild-type and tx-j) and between the two treatments (with or without maternal choline supplementation).

Mouse fetal liver WGBS and analysis

The same 16 samples used for RNA-seq were selected, each sample comprised of 6–9 pooled fetal livers from a single litter (Fetal Mouse WGBS Supplemental Table). DNA was isolated using the DNeasy Blood and Tissue Kit (QIAGEN), purity and integrity evaluated via NanoDrop spectrophotometer (Thermo Scientific) and agarose gel electrophoresis, and finally diluted with diethyl pyrocarbonate (DEPC)-treated water (Ambion) to a concentration of 10–20 ng/μl. Diluted DNA was bisulfite-converted using the EZ DNA Methylation Lightning kit (Zymo Research) according to the manufacturer's instructions. WGBS libraries were prepared using the TruSeq DNA Methylation kit (Illumina, Inc.) with indexed PCR primers and a 14-cycle PCR program. Libraries were sequenced at 4 per lane on the HiSeq2000 (Illumina, Inc.) at the Vincent J. Coates Genomics Sequencing Laboratory at UC Berkeley.

Reads without adaptors were aligned using BSseeker2 to the *mm10* reference sequence, then sorted with SAMtools. Reads containing adaptors were trimmed, aligned separately and sorted. Reads with and without adaptors were merged, PCR duplicates were removed and the bam files were converted to sam files using samtools. Sam files were converted to percent methylation bed files using custom Perl scripts. Quality was assessed through analysis of PCR duplicates, mappability and bisulfite conversion measured as 1% CHH methylation (Fetal Mouse WGBS Supplemental Table). Gene-specific methylation status was analyzed in promoter regions, defined as 5000 bases upstream to 1000 bases downstream of the transcription start site of each gene (32), determined as methylated over total reads at CpG dinucleotides for each sample.

Percent methylation bed files were converted to DSS format using a custom Perl script and DMRs for all pairwise comparisons between wild-type control and choline treatment, and tx-j control and choline treatment were identified using the bsseq R package (20) and DMRfinder tool (<https://github.com/cemordaunt/DMRfinder>). DMRs were further selected for those with a significant 10% methylation difference between groups and at least 10 reads per sample. Genome-wide significant DMRs were identified based on FWER < 0.05, determined by permuting the samples 1000 times by chromosome and counting the number of null permutations with equal or better DMRs ranked by number of CpGs and areaStat. Genes were assigned to DMRs by GREAT using the default basal plus extension parameters, except excluding curated regulatory domains (32). X and Y chromosome analyses were excluded since libraries were derived from pooled fetal livers with sexes combined. Code Availability: all code for WGBS data analysis is available on GitHub (<https://github.com/cemordaunt/WilsonDiseaseThioredoxin>).

Light microscopy and histology

Liver sections were stained with hematoxylin and eosin for histology. Slides were scanned using an Aperio Scanscope XT (Leica

Biosystems, Inc.) to produce digital whole slide images. Images were analyzed using Aperio Imagescope (Leica Biosystems, Inc.). Steatosis was graded 0 (<5%), 1 (6–33%), 2 (34–66%) and 3 (67–100%). Lobular and portal inflammation were graded on a four-point scale based on two or more inflammatory cells (foci) within close proximity to one another in a liver section viewed at 200X: grade 0 (none); 1 with 1–2 foci; 2 with 3–4 foci; 3 with >4 foci. Percentage of samples with inflammatory foci containing one or more neutrophils was determined. Fibrosis was graded 0 (none), 1 (expansion of portal fibrous tissue), 2 (early bridging, no nodules), 3 (bridging fibrosis, early nodule formation) and 4 (cirrhosis).

Plasma Alanine Transaminase

Plasma ALT levels were assessed using an enzymatic colorimetric assay from Bioo Scientific. ALT measurement was performed by the Mouse Metabolic Phenotyping Center at UC Davis.

Liver Protein Carbonyl

Liver protein carbonyl levels were assessed using a colorimetric assay from Cayman Chemical. Measurement was performed by the Mouse Metabolic Phenotyping Center at UC Davis.

Hepatic Copper and Iron quantification

Sections of liver (~180 mg) were digested with concentrated nitric acid and wet-ashed (9). Digested samples were diluted 10X with 18.2 MΩ-cm water prior to analysis by the Interdisciplinary Center for Plasma Mass Spectrometry at UC Davis using an Agilent 8900 ICP-MS (Agilent Technologies). Concentrations of copper and iron were quantified in single quad mode using a 0.4 mL/min MicroMist nebulizer to introduce samples and standards into a 2°C temperature-controlled spray chamber leading to a 1550 W plasma, with He or H₂ as the collision reaction cell gas. The external standards were diluted from Certiprep Multi-Element Solution 2A to 0.1 ppb, 0.5 ppb, 1 ppb, 5 ppb, 10 ppb, 50 ppb, 100 ppb, 500 ppb, 1000 ppb and 2500 ppb and the calibration range was extended for iron using CertiPrep Calibration Standard 3 diluted to 5 ppm, 10 ppm, 50 ppm and 100 ppm (SPEX CertiPrep Claritas). Standard dilutions were prepared using concentrated Trace Metals Grade HNO₃ (Fisher Scientific, Waltham, MA, USA) diluted to 5.4% with 18.2 MΩ-cm water. The samples and standards were introduced to the spray chamber at a 16.7:1 ratio to the internal standard. A NIST 1640a Trace Elements in Natural Water standard (National Institute of Standards and Technology, Gaithersburg, MD, USA) was analyzed initially, along with quality control standards 2A at 50 ppb and Calibration Standard 3 at 1000 ppb analyzed every 10th sample as quality controls. Values are expressed as μg/g liver.

Protein Isolation

Liver tissue (50 mg) was homogenized on ice in 500 μl of RIPA buffer containing protease and phosphatase inhibitors (Roche). The homogenate was incubated on ice for 20 minutes and then centrifuged at 4°C for 20 min at 10,600 g. Total protein was aliquoted and stored at –80°C until further use.

Western blot

Total protein concentration was calculated using the BCA assay kit (Pierce). Protein (50 μg) and Chameleon Duo pre-stained ladder (LI-COR, Inc.) were subjected to 4–20% precast polyacrylamide gels (Bio-Rad Laboratories, Inc.). The ladder

and samples were separated and wet-transferred onto 0.2 μ m low-fluorescence polyvinylidene difluoride membranes (Pierce) at 100 V. The membranes were dried for 1 h, reactivated in methanol and blocked in Odyssey Blocking Buffer PBS (LI-COR, Inc.) for 1 h. Primary antibodies were diluted in Odyssey Blocking Buffer (PBS) containing 0.2% Tween (Bio-Rad Laboratories, Inc.). Anti-TXN1 (1:500 dilution, Cell Signaling Technology, Inc.) was incubated at 4°C overnight and anti- β -actin (1:5,000 dilution, Sigma) was incubated for 1 h at room temperature. IRDye 800CW Donkey anti-Mouse IgG and IRDye 680RD Donkey anti-Goat IgG (1:20,000 dilution, LI-COR, Inc.) were used as secondary antibodies for imaging on the infrared Odyssey Imager (LI-COR, Inc.). TXN1 and β -actin bands were visualized at the expected sizes of ~12 kDa and 43 kDa against the ladder. Protein quantification was performed using the Odyssey infrared imaging software according to manufacturer's instructions.

ELISA for TXN

Liver TXN1 levels were assessed using a mouse ELISA assay from MyBioSource. Measurement was performed by the Mouse Metabolic Phenotyping Center at UC Davis.

Human liver biopsies

Samples were obtained from three sources: the University of Heidelberg in Heidelberg, Germany (WD); the California Pacific Medical Center, Ibrahim El-Hefni Biorepository in San Francisco, California, USA (WD and healthy control); the UC Davis GI biobank in Sacramento, California, USA (healthy control) (Human Liver WGBS Supplemental Table). Liver samples from the University of Heidelberg were derived from explanted livers from patients with WD who underwent liver transplant for acute liver failure or for cirrhosis and end-stage liver disease. Liver samples from the California Pacific Medical Center were obtained through percutaneous liver biopsies performed for diagnostic and staging purposes. Liver samples from the UC Davis GI biobank were obtained at the time of bariatric surgery from subjects without diabetes presenting <5% steatosis and no inflammation on histology.

All samples were de-identified, shipped on dry ice and stored at -80°C until further analysis. Informed written consent was obtained from each patient and the study protocol conformed to the ethical guidelines of the 1975 Declaration of Helsinki as reflected in a priori approval by the institutional review board at the University of California, Davis.

Human liver WGBS and analysis

DNA was isolated using the AllPrep RNA/DNA Micro Kit (QIAGEN), purity and integrity evaluated via NanoDrop spectrophotometer (Thermo Scientific) and agarose gel electrophoresis, and finally diluted in DEPC-treated water (Ambion) to achieve a concentration of 10–20 ng/ μ l. Diluted DNA was bisulfite-converted using the EZ DNA Methylation Lightning kit (Zymo Research) according to the manufacturer's instructions. WGBS libraries were prepared using the TruSeq DNA Methylation kit (Illumina, Inc.) with indexed PCR primers and a 14-cycle PCR program, and sequenced at 3–4 per lane on the HiSeq4000 (Illumina, Inc.). Sequencing was performed at the Vincent J. Coates Genomics Sequencing Laboratory at UC Berkeley.

Reads without adaptors were aligned using BSseeker2 to the hg38 reference sequence, then sorted with samtools. Reads containing adaptors were trimmed, aligned separately and

sorted. Reads with and without adaptors were merged, PCR duplicates were removed and the bam files were converted to sam files using samtools. Sam files were converted to percent methylation bed files using custom Perl scripts. Quality was assessed through analysis of PCR duplicates, mappability and bisulfite conversion measured as 1% CHH methylation (Human Liver WGBS Supplemental Table). WD-specific liver DMRs were obtained from (Mordaunt 2018). Genes were assigned to DMRs by GREAT using the default basal plus extension parameters, except excluding curated regulatory domains (32). Gene-specific methylation status was analyzed in promoter regions, defined as 5000 bases upstream to 1000 bases downstream of the transcription start site of each gene, determined as methylated over total reads at CpG dinucleotides for each sample. Code Availability: all code for WGBS data analysis is available on GitHub (<https://github.com/cemordaunt/WilsonDiseaseThioredoxin>). The data in this publication have been deposited in NCBI's Gene Expression Omnibus and are accessible through GEO series accession number GSE117592 (<https://www.ncbi.nlm.nih.gov/geo/query/acc.cgi?acc=GSE117592>).

Statistical analyses

Statistical analyses were performed using SPSS Statistics, version 23 (IBM), GraphPad Prism 6 (GraphPad Software) and R statistical software. For mouse data, differences were assessed with both sexes combined as well as males and females separately, and between sexes from the same group. Between group differences were assessed by one-way ANOVA (parametric) or Kruskal Wallis (non-parametric) with Tukey–Kramer *post hoc* test, with the exception of liver neutrophil data which was assessed using Fisher's exact test with Holm adjustment for multiple comparisons. Differences between sexes of mice from the same treatment group were assessed by two-tailed Student's *t*-test. In addition, the mean transcript levels of each gene were compared between treatment groups using ANCOVA, adjusting for hepatic iron as a covariate. Data are presented as mean \pm SEM. A $P < 0.05$ was considered significant. Spearman's correlations between any two variables were made using individual mouse data (i.e. if variable A was measured in a subset of 10 mice and variable B was measured in the entire treatment group, only mice used for variable A would be used to determine correlation between variables A and B).

For mouse TXN system promoter methylation and gene expression data, significance was assessed by two-way ANOVA with mouse genotype and choline treatment as independent variables, followed by Tukey's Honest Significant Difference *post hoc* test. For human TXN system promoter methylation data, significance was assessed by Student's *t*-test with diagnostic group as the independent variable. Significant differences were called if uncorrected $P < 0.05$.

Mouse genotype and choline treatment liver DMR methylation was associated with gene expression from RNA-seq data in the same samples. Genes were assigned to each DMR by GREAT and significance was assessed by linear regression. DMR-gene associations were called if uncorrected $P < 0.05$. Significant DMR-gene associations had FDR q -value < 0.05 . DMR-gene associations were further subset for genes with a significant (uncorrected $P < 0.05$) main effect of mouse genotype or treatment on expression in two-way ANOVA.

Overlap of human WD and mouse genotype and choline treatment DMR genes was determined by hypergeometric test compared to genes assigned to mouse background regions. Significant overlap was called if FDR q -value < 0.05 .

Supplementary Materials

Supplementary Materials are available at HMG online.

Acknowledgements

We would like to acknowledge the Ibrahim El Hefni Liver Biorepository at California Pacific Medical Center for providing human liver biopsies. We would also like to thank the UC Davis Mouse Biology Program and Mouse Metabolic Phenotyping Center for providing genotyping and metabolite assay services.

Conflict of Interest statement. None declared.

Funding

National Institutes of Health/NIDDK (grant numbers R03DK 099427 and R01DK104770); and Department and Divisional funds (awarded to V.M). V.M. is a full member of the University of California San Francisco Liver Center (Liver Center grant number P30 DK026743). The project described was supported by the National Center for Advancing Translational Sciences, National Institutes of Health, through grant number UL1 TR001860. The content is the sole responsibility of the authors and does not necessarily represent the official views of the National Institute of Health.

This work used the Vincent J. Coates Genomics Sequencing Laboratory at UC Berkeley, supported by NIH S10 Instrumentation (Grants S10RR029668 and S10RR027303).

References

- Åslund, F. and Beckwith, J. (1999) Bridge over troubled waters: sensing stress by disulfide bond formation. *Cell*, **96**, 751–753.
- Bernal, A.J., Dolinoy, D.C., Huang, D., Skaar, D.A., Weinhouse, C. and Jirtle, R.L. Adaptive radiation-induced epigenetic alterations mitigated by antioxidants. *FASEB J.* **27** (2): 665–71, 2013.
- Bestor, T.H. (1992) Activation of mammalian DNA methyltransferase by cleavage of a Zn binding regulatory domain. *EMBO J.*, **11**, 2611–2617.
- Board, F.N.M. (1998) Dietary reference intakes for thiamin, riboflavin, niacin, vitamin B6, folate, vitamin B12, pantothenic acid, biotin, and choline, a report of the Institute of Medicine Standing Committee on the Scientific Evaluation of Dietary Reference Intakes and its panel on folate, other B vitamins, and choline and subcommittee on upper reference levels of nutrients. National Academies Press, Washington DC.
- Cabras, T., Sanna, M., Manconi, B., Fanni, D., Demelia, L., Sorbello, O., Iavarone, F., Castagnola, M., Faa, G. and Messina, I. (2015) Proteomic investigation of whole saliva in Wilson's disease. *J. Proteomics*, **128**, 154–163.
- Caca, K., Ferenci, P., Kuhn, H.J., Polli, C., Willgerodt, H., Kunath, B., Hermann, W., Mossner, J. and Berr, F. (2001) High prevalence of the H1069Q mutation in East German patients with Wilson disease: rapid detection of mutations by limited sequencing and phenotype-genotype analysis. *J. Hepatol.*, **35**, 575–581.
- Cantoni, G.L. (1952) The nature of the active methyl donor formed enzymatically from l-methionine and adenosinetriphosphate₁. *J. Am. Chem. Soc.*, **74**, 2942–2943.
- Cassano, M., Offner, S., Planet, E., Piersigilli, A., Jang, S.M., Henry, H., Geuking, M.B., Mooser, C., McCoy, K.D., Macpherson, A.J. et al. (2017) Polyphenic trait promotes liver cancer in a model of epigenetic instability in mice. *Hepatology*, **66**, 235–251.
- Clegg, M.S., Keen, C.L., Lönnerdal, B. and Hurley, L.S. (1981) Influence of ashing techniques on the analysis of trace elements in animal tissue. *Biol. Trace Elem. Res.*, **3**, 107–115.
- Cohen, J.I., Roychowdhury, S., DiBello, P.M., Jacobsen, D.W. and Nagy, L.E. (2009) Exogenous thioredoxin prevents ethanol-induced oxidative damage and apoptosis in mouse liver. *Hepatology (Baltimore, Md)*, **49**, 1709–1717.
- Cope-Yokoyama, S., Finegold, M.J., Sturniolo, G.C., Kim, K., Mescoli, C., Rugge, M. and Medici, V. (2010) Wilson disease: histopathological correlations with treatment on follow-up liver biopsies. *World J. Gastroenterol.*, **16**, 1487–1494.
- Coronado, V., Naji, M. and Cox, D.W. (2001) The Jackson toxic milk mouse as a model for copper loading. *Mamm. Genome*, **12**, 793–795.
- Czlonkowska, A. and Litwin, T. (2017) Wilson disease - currently used anticopper therapy. *Handb. Clin. Neurol.*, **142**, 181–192.
- Detopoulou, P., Panagiotakos, D.B., Antonopoulou, S., Pitsavos, C. and Stefanadis, C. (2008) Dietary choline and betaine intakes in relation to concentrations of inflammatory markers in healthy adults: the ATTICA study. *Am. J. Clin. Nutr.*, **87**, 424–430.
- Ferenci, P., Weiss, K.H., Czlonkowska, A., Houwen, R., Szalay, F., Bruha, R., Stauber, R. and Stremmel, W. (2011) Gender Influences the Clinical Presentation of Wilson Disease (WD). *Gastroenterology*, **140**: S939–S939.
- Fischer, L.M., da Costa, K.A., Kwock, L., Stewart, P.W., Lu, T.S., Stabler, S.P., Allen, R.H. and Zeisel, S.H. (2007) Sex and menopausal status influence human dietary requirements for the nutrient choline. *Am. J. Clin. Nutr.* **85**: 1275–1285.
- Gromadzka, G., Schmidt, H.H.J., Genschel, J., Bochow, B., Rodo, M., Tarnacka, B., Litwin, T., Chabik, G. and Czlonkowska, A. (2006) p.H1069Q mutation in ATP7B and biochemical parameters of copper metabolism and clinical manifestation of Wilson's disease. *Mov. Disord.*, **21**, 245–248.
- Gu, M., Cooper, J.M., Butler, P., Walker, A.P., Mistry, P.K., Dooley, J.S. and Schapira, A.H. (2000) Oxidative-phosphorylation defects in liver of patients with Wilson's disease. *Lancet*, **356**, 469–474.
- Hall, A., Nelson, K., Poole, L.B. and Karplus, P.A. (2011) Structure-based insights into the catalytic power and conformational dexterity of peroxiredoxins. *Antioxid. Redox Signal.*, **15**, 795–815.
- Hansen, K.D., Langmead, B. and Irizarry, R.A. (2012) BSmooth: from whole genome bisulfite sequencing reads to differentially methylated regions. *Genome Biol.*, **13**, R83.
- Holliday, R. and Pugh, J.E. (1975) DNA modification mechanisms and gene activity during development. *Science*, **187**, 226–232.
- Jones, P.A. (2012) Functions of DNA methylation: islands, start sites, gene bodies and beyond. *Nat. Rev. Genet.*, **13**, 484–492.
- Li, M., Li, Y., Chen, J., Wei, W., Pan, X., Liu, J., Liu, Q., Leu, W., Zhang, L., Yang, X. et al. (2007) Copper ions inhibit S-adenosylhomocysteine hydrolase by causing dissociation of NAD⁺ cofactor. *Biochemistry*, **46**, 11451–11458.
- Liang, M. and Pietrusz, J.L. (2007) Thiol-related genes in diabetic complications: a novel protective role for endogenous thioredoxin 2. *Arterioscler. Thromb. Vasc. Biol.*, **27**, 77–83.
- Litwin, T., Gromadzka, G. and Czlonkowska, A. (2012) Gender differences in Wilson's disease. *J. Neurol. Sci.*, **312**, 31–35.

26. Liu, J., Morgan, M., Hutchison, K. and Calhoun, V.D. (2010) A study of the influence of sex on genome wide methylation. *PLOS ONE*, **5**, e10028.
27. Liu, Y., Qu, Y., Wang, R., Ma, Y., Xia, C., Gao, C., Liu, J., Lian, K., Xu, A., Lu, X. et al. (2012) The alternative crosstalk between RAGE and nitrative thioredoxin inactivation during diabetic myocardial ischemia-reperfusion injury. *Am. J. Physiol. – Endocrinol. Metab.* **303**, E841–E852.
28. Lu, J. and Holmgren, A. (2014) The thioredoxin antioxidant system. *Free Radic. Biol. Med.*, **66**, 75–87.
29. Lutsenko, S. (2014) Modifying factors and phenotypic diversity in Wilson's disease. *Ann. N.Y. Acad. Sci.*, **1315**, 56–63.
30. Mahmood, D.F., Abderrazak, A., El Hadri, K., Simmet, T. and Rouis, M. (2013) The thioredoxin system as a therapeutic target in human health and disease. *Antioxid. Redox Signal.*, **19**, 1266–1303.
31. Matsuo, Y. and Yodoi, J. (2013) Extracellular thioredoxin: a therapeutic tool to combat inflammation. *Cytokine Growth Factor Rev.*, **24**, 345–353.
32. McLean, C.Y., Bristor, D., Hiller, M., Clarke, S.L., Schaar, B.T., Lowe, C.B., Wenger, A.M. and Bejerano, G. (2010) GREAT improves functional interpretation of cis-regulatory regions. *Nat. Biotechnol.*, **28**, 495–501.
33. Medici, V., Kieffer, D.A., Shibata, N.M., Chima, H., Kim, K., Canovas, A., Medrano, J.F., Islas-Trejo, A.D., Kharbanda, K.K., Olson, K. et al. (2016) Wilson disease: epigenetic effects of choline supplementation on phenotype and clinical course in a mouse model. *Epigenetics* **11**, 804–818.
34. Medici, V., Shibata, N.M., Kharbanda, K.K., Islam, M.S., Keen, C.L., Kim, K., Tillman, B., French, S.W., Halsted, C.H. and LaSalle, J.M. (2014) Maternal choline modifies fetal liver copper, gene expression, DNA methylation, and neonatal growth in the tx-j mouse model of Wilson disease. *Epigenetics*, **9**, 286–296.
35. Medici, V., Shibata, N.M., Kharbanda, K.K., LaSalle, J.M., Woods, R., Liu, S., Engelberg, J.A., Devaraj, S., Török, N.J., Jiang, J.X. et al. (2013) Wilson disease: changes in methionine metabolism and inflammation affect global DNA methylation in early liver disease. *Hepatology* **57**, 555–565.
36. Mehta, A.K., Singh, B.P., Arora, N. and Gaur, S.N. (2010) Choline attenuates immune inflammation and suppresses oxidative stress in patients with asthma. *Immunobiology*, **215**, 527–534.
37. Mihaylova, V., Todorov, T., Jeleu, H., Kotsev, I., Angelova, L., Kosseva, O., Georgiev, G., Ganeva, R., Cherninkova, S., Tankova, L., Savov, A. and Tournev, I. (2012) Neurological symptoms, genotype-phenotype correlations and ethnic-specific differences in Bulgarian patients with Wilson disease. *Neurologist*, **18**, 184–189.
38. Mortazavi, A., Williams, B.A., McCue, K., Schaeffer, L. and Wold, B. (2008) Mapping and quantifying mammalian transcriptomes by RNA-Seq. *Nat. Methods*, **5**, 621–628.
39. Nagasaka, H., Inoue, I., Inui, A., Komatsu, H., Sogo, T., Murayama, K., Murakami, T., Yorifuji, T., Asayama, K., Katayama, S. et al. (2006) Relationship between oxidative stress and antioxidant systems in the liver of patients with Wilson disease: hepatic manifestation in Wilson disease as a consequence of augmented oxidative stress. *Pediatr. Res.* **60**, 472–477.
40. Niculescu, M.D. and Zeisel, S.H. (2002) Diet, methyl donors and DNA methylation: interactions between dietary folate, methionine and choline. *J. Nutr.*, **132**, 2333S–2335S.
41. Niedzwiecki, M.M., Liu, X., Hall, M.N., Thomas, T., Slavkovich, V., Ilievski, V., Levy, D., Alam, S., Siddique, A.B., Parvez, F., Graziano, J.H. and Gamble, M.V. (2015) Sex-specific associations of arsenic exposure with global DNA methylation and hydroxymethylation in leukocytes: results from two studies in Bangladesh. *Cancer Epidemiol. Biomarkers Prev.*, **24**, 1748–1757.
42. Okano, M., Bell, D.W., Haber, D.A. and Li, E. (1999) DNA methyltransferases Dnmt3a and Dnmt3b are essential for de novo methylation and mammalian development. *Cell*, **99**, 247–257.
43. Prinz, W.A., Aslund, F., Holmgren, A. and Beckwith, J. (1997) The role of the thioredoxin and glutaredoxin pathways in reducing protein disulfide bonds in the *Escherichia coli* cytoplasm. *J. Biol. Chem.*, **272**, 15661–15667.
44. Riordan, S.M. and Williams, R. (2001) The Wilson's disease gene and phenotypic diversity. *J. Hepatol.*, **34**, 165–171.
45. Scheinberg, I.H. and Sternlieb, I. (1965) Wilson's Disease. *Annu. Rev. Med.*, **16**, 119–134.
46. Seessle, J., Gohdes, A., Gotthardt, D.N., Pfeiffenberger, J., Eckert, N., Stremmel, W., Reuner, U. and Weiss, K.H. (2011) Alterations of lipid metabolism in Wilson disease. *Lipids Health Dis.*, **10**, 83.
47. Stattermayer, A.F., Traussnigg, S., Dienes, H.P., Aigner, E., Stauber, R., Lackner, K., Hofer, H., Stift, J., Wrba, F., Stadlmayr, A. et al. (2015) Hepatic steatosis in Wilson disease—Role of copper and PNPLA3 mutations. *J. Hepatol.*, **63**, 156–163.
48. Sternlieb, I. (1968) Mitochondrial and fatty changes in hepatocytes of patients with Wilson's disease. *Gastroenterology*, **55**, 354–367.
49. Tomat, A.L. and Salazar, F.J. (2014) Mechanisms involved in developmental programming of hypertension and renal diseases. Gender differences. *Horm. Mol. Biol. Clin. Investig.*, **18**, 63–77.
50. Weiss, K.H., Gotthardt, D.N., Klemm, D., Merle, U., Ferenci-Foerster, D., Schaefer, M., Ferenci, P. and Stremmel, W. (2011) Zinc monotherapy is not as effective as chelating agents in treatment of Wilson disease. *Gastroenterology*, **140**, 1189–1198.e1181.
51. Wickramasinghe, S., Rincon, G., Islas-Trejo, A. and Medrano, J.F. (2012) Transcriptional profiling of bovine milk using RNA sequencing. *BMC Genomics*, **13**, 1471–2164.
52. Wilson, S.L., Liu, Y. and Robinson, W.P. (2016) Placental telomere length decline with gestational age differs by sex and TERT, DNMT1, and DNMT3A DNA methylation. *Placenta*, **48**, 26–33.
53. Wu, Y., Bu, F., Yu, H., Li, W., Huang, C., Meng, X., Zhang, L., Ma, T. and Li, J. (2017) Methylation of Septin9 mediated by DNMT3a enhances hepatic stellate cells activation and liver fibrogenesis. *Toxicol. Appl. Pharmacol.*, **315**, 35–49.
54. Yoshihara, E., Masaki, S., Matsuo, Y., Chen, Z., Tian, H. and Yodoi, J. (2014) Thioredoxin/Txnip: redoxosome, as a redox switch for the pathogenesis of diseases. *Front. Immunol.*, **4**, 1–9.
55. Zeisel, S.H. and da Costa, K-A. (2009) Choline: an essential nutrient for public health. *Nutr. Rev.* **67**, 615–623.
56. Zischka, H., Lichtmannegger, J., Schmitt, S., Jagemann, N., Schulz, S., Wartini, D., Jennen, L., Rust, C., Larochette, N., Galluzzi, L. et al. (2011) Liver mitochondrial membrane crosslinking and destruction in a rat model of Wilson disease. *J. Clin. Invest.* **121**, 1508–1518.